

Reconstructing the invisible with matrix elements

Danilo Enoque Ferreira de Lima*

Physikalisches Institut, Ruprechts-Karls-Universität Heidelberg, 69120 Heidelberg, Germany

Olivier Mattelaer†

*Centre for Cosmology, Particle Physics and Phenomenology (CP3/IRMP)
Université Catholique de Louvain, 1348 Louvain-la-neuve, Belgium*

Michael Spannowsky‡

*Institute for Particle Physics Phenomenology, Department of Physics, Durham University, Durham DH1 3LE, U.K.
(Dated: December 12, 2017)*

INTRODUCTION

The extraction of few interesting signal events from a large number of Standard Model background events is one of the biggest challenges at the Large Hadron Collider (LHC). Depending on the nature and kinematic topology of the signal, different techniques and strategies have been devised to perform this task.

In general, in a first step, observables that are characteristic to the signal have to be constructed. This could entail simple observables, like the transverse momentum of reconstructed objects, e.g. leptons, photons or jets, or the total amount of missing energy, or more sophisticated observables, like jet substructure observables. If the signal is a heavy resonance that decays into electroweak gauge bosons or the top quark, which in turn have a large branching ratio into jets, studying the substructure of jets is a popular way to separate them from large QCD backgrounds [1, 2]. Either kind of observables can then be further processed using increasingly popular multivariate analysis (MVA) techniques, e.g. neural nets or boosted decision trees, to perform an hypothesis test between signal and background.

An alternative way of performing an hypothesis test is to use the measured particles' momenta as direct input to the evaluation of the matrix element of the assumed underlying process, thereby evaluating if the final state was more likely to be produced by the signal or background hypothesis. This approach is called Matrix Element Method (MEM) [3–5]. As it is based on an analytic calculation of the process, this method can be directly applied to data and does not require training on Monte-Carlo-generated pseudo-data.

However, while MEM has been used very successfully in a wider range of applications and measurements [4, 6–9], and recent developments extended it to the substructure of jets [10, 11], next-to-leading order accuracy [12–15] and even to an arbitrary number of reconstructed final state objects [16, 17], as an all-information approach, it always had its shortcomings when multiple invisible objects are present in the final state.

Here, we propose a fully flexible method to perform an hypothesis test between signal and background based on the Matrix Element Method in the presence of multiple invisible particles. The method performs a mapping of the measured final state onto its minimal hypersurface of degrees of freedom for a given process. It then maximises the matrix element on this hypersurface separately for signal and background. On the one hand, this allows to make an educated guess of the 4-momenta of the invisible particles in the process, and on the other hand it allows to construct a variable χ as the ratio of the matrix elements that can be used to separate signal from backgrounds.

Final states with multiple missing energy particles became an increasingly important signature in searches for a plethora of new physics scenarios at the LHC, e.g. searches for dark matter [18, 19], R-parity conserving supersymmetry [20, 21], large extra dimensions [22], or even anomalous couplings of the Higgs boson [23, 24]. Thus, a flexible method not relying on Monte-Carlo-generated pseudo-data can be readily applied to ongoing searches and measurements at the LHC's multipurpose experiments and increase their discovery potential.

DESCRIPTION OF THE METHOD

The matrix element method assigns probabilities to signal and background for each event of a sample. The most attractive feature of this method is that it makes maximal use of both the experimental information and the theoretical model. It associates a weight to each event based on the value of the matrix element (*i.e.*, the scattering amplitude) for that specific final state configuration for each of the hypotheses. The weight associated with an experimental event x , given a set of hypotheses α , is

$$P_\alpha(x) = \frac{1}{\sigma_\alpha} \int d\Phi(y) |M_\alpha|^2(y) W(x, y), \quad (1)$$

where $|M_\alpha|^2(y)$ is the squared leading-order matrix element, $d\Phi(y)$ is the phase-space measure, (including the

parton distribution functions) and $W(x, y)$ is the transfer function which describes the evolution of the final state parton-level configuration in y into a reconstructed event x in the detector. The normalization by the total cross section σ_α in Eq. (1) ensures that $P_\alpha(x)$ is a probability density, $\int P_\alpha(x) dx = 1$, if the transfer function is normalized to one. As is evident from the definition in Eq. (1), the calculation of each weight involves a non-trivial multi-dimensional integration of complicated functions over the phase space. Even if the problem of computing the weights for arbitrary models and processes can be automated, e.g. as implemented in MADWEIGHT [5], such calculations remain extremely CPU intensive and are subject to numerical inaccuracies. We instead propose to replace the convolution of the matrix element with the transfer function by a maximisation procedure over the phase-space volume Φ ,

$$w_\alpha(x) = \max_{y \in \Phi} (|M_\alpha|^2(y)W(x, y)). \quad (2)$$

In order to use efficiently the maximization algorithms over a highly dimensional space, it is important to parametrize the phase-space in an optimal way. In particular, the invariant mass of every propagator that can be on-shell needs to be used as a degree of freedom of the phase-space, as well as all the angles of visible particles (due to the high detector resolution on those quantities). Such parametrization allows to reduce the variance of the function by smoothing the peak and it helps to find its maximum more efficiently. We rely on MADWEIGHT to find such a parametrization, which provides a large set of changes of variables that can be combined to reach the optimal parametrization of the phase-space.

After finding the most likely final state configuration, given a limited amount of information¹, we construct an observable χ , which classifies each event on whether it appears more signal- or background-like:

$$\log(\chi) = \log\left(\frac{w_S}{\sum_i w_{B_i}}\right). \quad (3)$$

The significant gain in speed and high performance of the classifier, allows one to extend it to complex final states with many objects. The method can be integrated straightforwardly into the EVENTDECONSTRUCTION approach [16], thereby extending EVENTDECONSTRUCTION, which was already designed to handle an arbitrary number of visible final state objects, to final states with invisible particles.

Thus, even if this letter focuses on a single example, the method is entirely generic and can be applied to a large class of analyses. We will release a generic code [25],

¹ That is, only the visible final state, which can be plagued by experimental uncertainties.

which allows to apply the above method efficiently for any process and set of transfer functions, hence providing the same flexibility as MADWEIGHT.

PARTLY INVISIBLE HIGGS BOSON RECONSTRUCTION

To show how performant the method is in separating signal from background, we apply it to the prominent partly invisible decay of a Higgs boson into a muon-antimuon pair and two muon-neutrinos via two W bosons [26–28]. The $pp \rightarrow H \rightarrow W^+W^- \rightarrow \mu^+\nu_\mu\mu^-\bar{\nu}_\mu$ signal and dominant background [29], $pp \rightarrow W^+W^- \rightarrow \mu^+\nu_\mu\mu^-\bar{\nu}_\mu$, have been simulated using MadGraph5_aMC@NLO 2.5.2 [30, 31] and showered with Pythia 8.226 [32], thereby allowing for hadronisation effects and additional initial state radiation. We assume an integrated luminosity of 30 fb^{-1} and simulate proton-proton collisions at $\sqrt{s} = 13 \text{ TeV}$.

Before we apply the matrix-element-method, we select candidate events with the following event selection cuts, which render all but one irreducible background process insignificant. We select muons with a minimum transverse momentum requirement of $p_{T,\mu} > 10 \text{ GeV}$ and a requirement that the absolute value of the pseudo-rapidity is $|\eta_\mu| < 2.5$, to ensure that the muons are within the range of the detector’s tracker system. The experimental resolution on the momenta of the muons are precise enough for us to assume their experimental uncertainty to be negligible. Thus, we define $W(x, y)$ of Eq. 2 as $W(x, y) = \delta^4(p_{\mu^+}^{exp} - p_{\mu^+}^{MC})\delta^4(p_{\mu^-}^{exp} - p_{\mu^-}^{MC})$. To reduce the muon mis-identification rate, the sum I of charged particles within $\Delta R(\mu, \text{particle}) < \min(0.3, 10 \text{ GeV}/p_T^\mu)$ has been required to satisfy $I/p_T^\mu < 0.06$.

	Signal	Background	s/b	s/\sqrt{b}
Basic event selection cuts	327	11451	0.029	3.058
Assuming perfect E_T^{miss} reconstruction				
Veto $\chi_{S,B}(S, B) = 0$	299	3724	0.080	4.912
$\log(\chi) > 1$	262	2200	0.119	5.592
$\log(\chi) > 1.5$	118	808	0.146	4.157
Assuming a 10% resolution effect in E_T^{miss}				
Veto $w_{S,B}(S, B) = 0$	294	3742	0.079	4.806
$\log(\chi) > 1$	256	2204	0.116	5.455
$\log(\chi) > 1.5$	114	811	0.141	4.016

TABLE I. Signal-to-background ratio and signal-to-square-root-of-background ratio after basic selection and the proposed method.

With these basic selection cuts, for $\sqrt{s} = 13 \text{ TeV}$ and an integrated luminosity of $L = 30 \text{ fb}^{-1}$, and no detector simulation, we obtain a signal-to-background ratio of $S/B \simeq 0.03$ and a statistical sensitivity of $S/\sqrt{B} \simeq 3.06$, as shown in Table I.

For the signal pseudo-data generated, we can now use the method discussed to evaluate the weight for a sig-

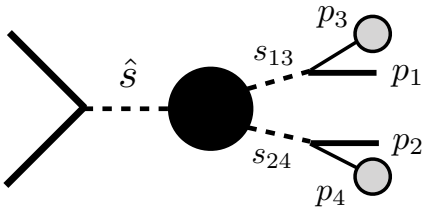
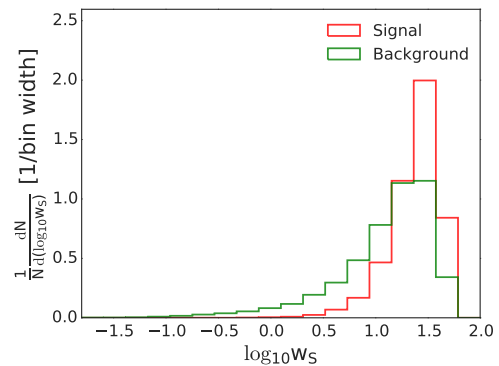


FIG. 1. Kinematic for signal and background processes.

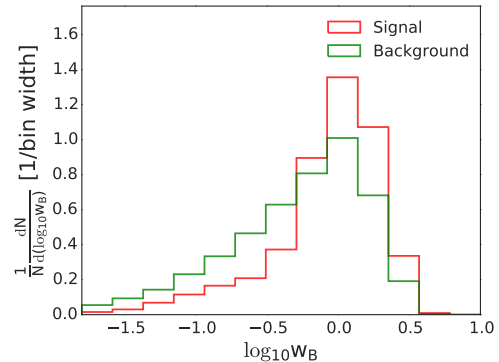
nal event to look like signal $w_S(S)$ or to look like background $w_B(S)$. The impact of initial state radiation is dampened by implementing a boost back technique of the reconstructed momenta of the lepton as suggested in [6]. The four free parameters defining the phase space Φ over which we maximise the matrix elements are \hat{s} , s_{13} , s_{24} , as shown in Fig. 1, and the rapidity of the full system y_{all} , where all includes the two muons and the missing transverse energy. In the example at hand, we can impose further boundary conditions, i.e. $\sqrt{\hat{s}} \simeq m_h$, $\sqrt{s_{13}} \simeq m_W$ and $\sqrt{s_{24}} < m_W$ for the signal and $2m_W < \sqrt{\hat{s}} < 3m_W$, $\sqrt{s_{13}} \simeq m_W$ and $\sqrt{s_{24}} \simeq m_W$ for the background². Despite limiting the four-dimensional parameter space, the matrix-element weighted hypersurface is complicated enough to give rise to multiple minima or to fail to give a physical solution for the matrix element entirely. Thus, to find the global minimum we rerun the minimisation procedure with randomly modified initial conditions $n_r = 500$ times for signal and background each³.

Thus, we can calculate the weight for the signal and background hypotheses w_S and w_B , respectively for signal and background events. We show all four distributions in Figs. 2(a) and 2(b). Event kinematics which do not result in a physical configuration for the signal or background hypothesis give either $w_S = 0$ or $w_B = 0$. We do not show such events in Figs. 2(a) and 2(b), but their fraction can be inferred from Table I. A fairly large number of background events fail to pass the kinematic requirements to look like signal, i.e. resulting in $w_S(B) = 0$. This behaviour is beneficial for the significance of the analysis, as such background events have zero probability to mimic the signal.

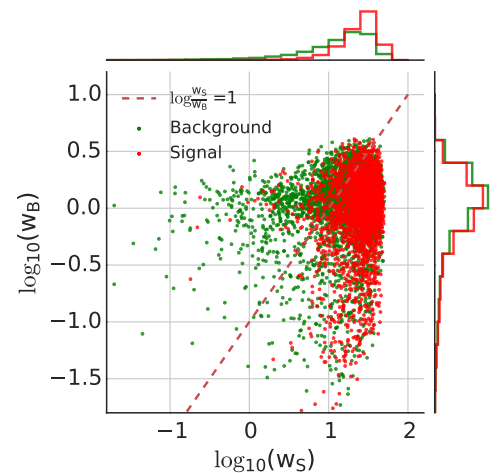
After vetoing all events where $w_{S,B}(S,B) = 0$ we find $S/B = 0.08$, $S/\sqrt{B} \simeq 4.81$ and show the distribution of weights in Fig. 2(c). While a comparison of the absolute weights for the signal and background hypothesis does



(a)



(b)



(c)

FIG. 2. Signal (w_S) and background (w_B) weight distributions for signal (red) and background (green) samples respectively.

not allow for a strong separation on an event-by-event basis (see the distributions on the horizontal and vertical axes of Fig. 2(c)), taking the ratio

$$\chi = \frac{w_S}{w_B} \quad (4)$$

for each event results in a strong discrimination between

² We tested larger windows for $\sqrt{\hat{s}}$ but did not find them to change the background weights significantly. The asymmetric phase-space cuts on $\sqrt{s_{13}}$ and $\sqrt{s_{24}}$ are flipped half of the time when maximizing over the phase space.

³ We have varied n_r between 0 and 500 and find for $n_r > 150$ the change of w_S and w_B to be insignificant.

signal and background, see Fig. 3. For example, by requiring $\log(\chi) \geq 1$ we reject 81% of background while still accepting 80% of signal, resulting in $S/B \simeq 0.12$ and $S/\sqrt{B} \simeq 5.59$. We show the full ROC curve for a variable cut on $\log(\chi)$ in Fig. 4.

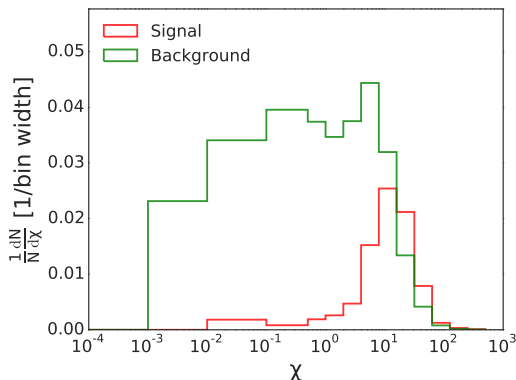


FIG. 3. Distribution of χ for signal (red) and background (green).

While the momenta of the charged leptons can be measured very precisely, the total amount of missing transverse energy instead is subject to experimental uncertainties. Such uncertainties can potentially affect the ROC curve and overall significance negatively. To estimate the impact of this uncertainty on our method we include a 10% resolution effect by smearing the missing energy with a gaussian distribution.

Both in the ROC curve and Table I, we show the effect of the resolution effect on the missing transverse energy for this method. We find however, that such effect reduces s/\sqrt{b} only slightly from 5.59 to 5.46.

Instead of a cut and count procedure, one can use the full shape of the $\log(\chi)$ distribution of Fig. 3 to set a CLs [33, 34] limits on the Higgs-W coupling. Including the 10% resolution effect on the missing transverse energy reconstruction, one can set a 95% CL limit on the Higgs-W-boson coupling at $g_{H,WW} \in [0.65, 1.25] \times g_{H,WW,SM}$. While a direct comparison is difficult due to the different collider energies, the limit we obtain is already better than the one from the full combined 7 and 8 TeV data set for the gluon-fusion Higgs production process with subsequent decay into W bosons [35].

SUMMARY AND CONCLUSION

We have proposed a matrix-element method, designed to perform a hypothesis-test in the presence of multiple invisible particles in the final state. Without integrating over the phase space the most-likely kinematic configuration is calculated separately for signal and background. We make full use of the information available on the particle involved in the process.

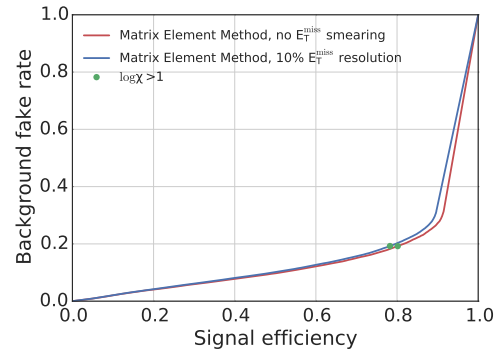


FIG. 4. Background mis-identification rate versus signal efficiency for the proposed method, with (blue) and without (red) smearing of the missing transverse energy.

We applied this method to separate the process $pp \rightarrow H \rightarrow WW^* \rightarrow \mu^+\mu^-\nu_\mu\bar{\nu}_\mu$ from the irreducible background $pp \rightarrow WW \rightarrow \mu^+\mu^-\nu_\mu\bar{\nu}_\mu$. Using only objects that are experimentally well under control, i.e. the momenta of the muons, from which we calculate the missing transverse energy, we are able to set a strong limit on the Higgs-coupling to W bosons, assuming an integrated luminosity of 30 fb^{-1} at $\sqrt{s} = 13 \text{ TeV}$.

Other methods to reconstruct partly invisible final states have been devised before, e.g. m_{T2} [9, 36] or boosted kinematics [37]. However, this matrix element method is not relying on a specific kinematic structure for the decays, e.g. the presence of particles with the same mass, or the number of invisible final state particles. We will release a generic Monte-Carlo implementation of this method in a future publication [25], thereby showing the flexibility and applicability to a wide range of beyond the Standard Model scenarios.

Acknowledgements:

OM would like to thank Pierre Artoisenet for fruitful discussions and the CERN TH division for its hospitality. OM was partly supported by the Belgian Pole d'attraction Inter-Universitaire (PAI P7/37) and by the European Union's Horizon 2020 research and innovation programme as part of the Marie Skłodowska-Curie Innovative Training Network MC-netITN3 (grant agreement no. 722104). DEFL has been partly supported by the Alexander von Humboldt Foundation.

* dferreir@cern.ch

† olivier.mattelaer@uclouvain.be

‡ michael.spannowsky@durham.ac.uk

[1] A. Abdesselam *et al.*, *Boost 2010 Oxford, United Kingdom, June 22-25, 2010*, *Eur. Phys. J. C* **71**, 1661 (2011), arXiv:1012.5412 [hep-ph].

- [2] A. Altheimer *et al.*, *BOOST 2011 Princeton*, NJ, USA, 22-26 May 2011, *J. Phys.* **G39**, 063001 (2012), [arXiv:1201.0008 \[hep-ph\]](#).
- [3] K. Kondo, *J. Phys. Soc. Jap.* **57**, 4126 (1988).
- [4] V. M. Abazov *et al.* (D0), *Nature* **429**, 638 (2004), [arXiv:hep-ex/0406031 \[hep-ex\]](#).
- [5] P. Artoisenet, V. Lemaître, F. Maltoni, and O. Mattelaer, *JHEP* **12**, 068 (2010), [arXiv:1007.3300 \[hep-ph\]](#).
- [6] J. Alwall, A. Freitas, and O. Mattelaer, *Phys. Rev.* **D83**, 074010 (2011), [arXiv:1010.2263 \[hep-ph\]](#).
- [7] J. R. Andersen, C. Englert, and M. Spannowsky, *Phys. Rev.* **D87**, 015019 (2013), [arXiv:1211.3011 \[hep-ph\]](#).
- [8] P. Artoisenet, P. de Aquino, F. Maltoni, and O. Mattelaer, *Phys. Rev. Lett.* **111**, 091802 (2013), [arXiv:1304.6414 \[hep-ph\]](#).
- [9] A. Betancur, D. Debnath, J. S. Gainer, K. T. Matchev, and P. Shyamsundar, (2017), [arXiv:1708.07641 \[hep-ph\]](#).
- [10] D. E. Soper and M. Spannowsky, *Phys. Rev.* **D84**, 074002 (2011), [arXiv:1102.3480 \[hep-ph\]](#).
- [11] D. E. Soper and M. Spannowsky, *Phys. Rev.* **D87**, 054012 (2013), [arXiv:1211.3140 \[hep-ph\]](#).
- [12] J. M. Campbell, W. T. Giele, and C. Williams, *JHEP* **11**, 043 (2012), [arXiv:1204.4424 \[hep-ph\]](#).
- [13] J. M. Campbell, R. K. Ellis, W. T. Giele, and C. Williams, *Phys. Rev.* **D87**, 073005 (2013), [arXiv:1301.7086 \[hep-ph\]](#).
- [14] T. Martini and P. Uwer, *JHEP* **09**, 083 (2015), [arXiv:1506.08798 \[hep-ph\]](#).
- [15] A. V. Gritsan, R. Rntsch, M. Schulze, and M. Xiao, *Phys. Rev.* **D94**, 055023 (2016), [arXiv:1606.03107 \[hep-ph\]](#).
- [16] D. E. Soper and M. Spannowsky, *Phys. Rev.* **D89**, 094005 (2014), [arXiv:1402.1189 \[hep-ph\]](#).
- [17] C. Englert, O. Mattelaer, and M. Spannowsky, *Phys. Lett.* **B756**, 103 (2016), [arXiv:1512.03429 \[hep-ph\]](#).
- [18] M. Aaboud *et al.* (ATLAS), (2017), [arXiv:1711.03301 \[hep-ex\]](#).
- [19] A. M. Sirunyan *et al.* (CMS), *JHEP* **03**, 061 (2017), [Erratum: *JHEP*09,106(2017)], [arXiv:1701.02042 \[hep-ex\]](#).
- [20] A. M. Sirunyan *et al.* (CMS), (2017), [arXiv:1710.09154 \[hep-ex\]](#).
- [21] M. Aaboud *et al.* (ATLAS), (2017), [arXiv:1711.01901 \[hep-ex\]](#).
- [22] S. Chatrchyan *et al.* (CMS), *Phys. Rev. Lett.* **108**, 261803 (2012), [arXiv:1204.0821 \[hep-ex\]](#).
- [23] M. Aaboud *et al.* (ATLAS), (2017), [arXiv:1708.09624 \[hep-ex\]](#).
- [24] V. Khachatryan *et al.* (CMS), *JHEP* **02**, 135 (2017), [arXiv:1610.09218 \[hep-ex\]](#).
- [25] D. Ferreira de Lima, O. Mattelaer, and M. Spannowsky, “In preparation,”.
- [26] M. Dittmar and H. K. Dreiner, *Phys. Rev.* **D55**, 167 (1997), [arXiv:hep-ph/9608317 \[hep-ph\]](#).
- [27] V. Khachatryan *et al.* (CMS), *JHEP* **03**, 032 (2017), [arXiv:1606.01522 \[hep-ex\]](#).
- [28] G. Aad *et al.* (ATLAS), *Phys. Rev.* **D92**, 012006 (2015), [arXiv:1412.2641 \[hep-ex\]](#).
- [29] S. Chatrchyan *et al.* (CMS), *JHEP* **01**, 096 (2014), [arXiv:1312.1129 \[hep-ex\]](#).
- [30] J. Alwall, R. Frederix, S. Frixione, V. Hirschi, F. Maltoni, O. Mattelaer, H. S. Shao, T. Stelzer, P. Torrielli, and M. Zaro, *JHEP* **07**, 079 (2014), [arXiv:1405.0301 \[hep-ph\]](#).
- [31] V. Hirschi and O. Mattelaer, *JHEP* **10**, 146 (2015), [arXiv:1507.00020 \[hep-ph\]](#).
- [32] T. Sjostrand, S. Mrenna, and P. Z. Skands, *Comput. Phys. Commun.* **178**, 852 (2008), [arXiv:0710.3820 \[hep-ph\]](#).
- [33] G. J. Feldman and R. D. Cousins, *Phys. Rev.* **D57**, 3873 (1998), [arXiv:physics/9711021 \[physics.data-an\]](#).
- [34] T. Junk, *Nucl. Instrum. Meth.* **A434**, 435 (1999), [arXiv:hep-ex/9902006 \[hep-ex\]](#).
- [35] G. Aad *et al.* (ATLAS), *Eur. Phys. J.* **C76**, 6 (2016), [arXiv:1507.04548 \[hep-ex\]](#).
- [36] C. G. Lester and D. J. Summers, *Phys. Lett.* **B463**, 99 (1999), [arXiv:hep-ph/9906349 \[hep-ph\]](#).
- [37] C. Englert, M. Spannowsky, and C. Wymant, *Phys. Lett.* **B718**, 538 (2012), [arXiv:1209.0494 \[hep-ph\]](#).